Response of CdWO$_4$ crystal scintillator for few MeV ions and low energy electrons

P.G. Bizzeti [a], L. Carraresi [a], F.A. Danevich [b], T. Fazzini [a], P.R. Maurenzig [a], F. Taccetti [a], N. Taccetti [a], V.I. Tretyak [b],*

[a] Dipartimento di Fisica, Universita di Firenze and INFN sez. Firenze, I-50019, Italy
[b] Institute for Nuclear Research, MSP 03680 Kyiv, Ukraine

ABSTRACT

The response of a CdWO$_4$ crystal scintillator to protons, α particles, Li, C, O and Ti ions with energies in the range 1–10 MeV was measured. The non-proportionality of CdWO$_4$ for low energy electrons (4–110 keV) was studied with the Compton Coincidence Technique. The energy dependence of the quenching factors for ions and the relative light yield for low energy electrons was calculated using a semi-empirical approach. Pulse-shape discrimination ability between γ quanta, protons, α particles and ions was investigated.

© 2012 Elsevier B.V. All rights reserved.

1. Introduction

Numerous astronomical and cosmological observations since 1930s suggest that most of the matter in the Universe is non-luminous and non-baryonic, while usual matter constitutes only $\simeq 4\%$ of the Universe and the main components are dark matter ($\simeq 23\%$) and dark energy ($\simeq 73\%$) [1,2]. Dark matter (DM) is preferably related to particles that are neutral and only weakly interacting with matter (Weakly Interacting Massive Particles, WIMPs). Interaction of such particles with usual matter could be detected through the observation of nuclear recoils created after scattering of WIMPs on atomic nuclei in sensitive detectors placed in low background conditions deep underground. Positive evidence of WIMPs observation at $\simeq 9\sigma$ confidence level is reported in the DAMA experiment [3] after 13-year measurements with large mass low background NaI(Tl) scintillators. This result was recently supported by the CoGeNT [4] and CRESST [5] data. However, many other searches for WIMPs to-date gave only negative results [6,7]. Because of the fundamental importance of the question of the DM constituents, searches for WIMPs are under performance or planned in near 20 experiments, in particular, in the ton-scale projects

EURECA with cryogenic Ge and different crystal scintillating bolometers [8], DARWIN with scintillating noble gases [9] and DAMA/1 ton (proposed since 1996) [10].

When the energy released by the recoil ions is measured with scintillators, one of the main questions is the quenching of the scintillation light yield. Since a long time it is known that the amount of light produced in scintillating materials by highly ionising particles is lower than that produced by electrons of the same energy [11]. In a scintillator calibrated with γ sources, signals from ions will be seen at lower energies than their real values, sometimes by more than one order of magnitude. Knowledge of quenching factor, QF (i.e. ratio of the measured ion energy in γ scale to its real energy) is very important in searches for WIMPs and in predictions where the WIMPs signal should be expected. QFs depend on many factors such as the scintillating material itself, its dopants and impurities, temperature; ion's Z and A numbers, ion's energy; time of collection of scintillating signal, etc. (see some examples in Ref. [12]). Since it is sometimes quite difficult to measure QFs for the needed ions and in the needed energy region (f.e. for low-energy heavy ions when the scintillation signal is expected at $\simeq 10$ keV or less), some methods for the QFs estimation are of great interest.

QFs for different ions in a scintillator could be not independent but related quantities. Such a hypothesis, supported by some experimental data, was discussed already in Ref. [11]. If true, on the basis of measurements of QFs for particles of one kind in some

energy region (e.g. for a few MeV α particles from internal contamination of a detector), one would be able to *calculate* QFs for particles of another kind and for other energies (e.g. for low energy nuclear recoils). Further evidences in favour of this hypothesis were given in Ref. [12].

Cadmium tungstate (CdWO$_4$) crystal scintillators are widely used in low counting experiments to search for 2β decay [13–17] and studies of rare β [18,19] and α [20] decays. CdWO$_4$ has rather similar properties to CaWO$_4$, ZnWO$_4$, CaMoO$_4$ and some other oxide crystal scintillators, promising targets for DM experiments [8].

In this work we measured the response of a CdWO$_4$ crystal to few MeV energy ions and low energy (4–110 keV) electrons. Pulse-shape discrimination ability was studied for protons, α particles, Li, C, O and Ti ions. Using the measured quenching for protons, we applied a semi-empirical approach [12] to calculate QFs for other ions and low energy electrons.

2. Crystal characteristics and signal processing

The CdWO$_4$ crystal studied in this work is a parallelepiped of $10 \times 20 \times 25$ mm, manufactured by Scionix. CdWO$_4$ is a monoclinic, almost orthorhombic, crystal. From the specification of the manufacturer, the 10×20 mm faces are known to be cleavage (010) planes. Measurements performed with a diffractometer[1] confirm this assignment, while the two faces 10×25 mm and 20×25 mm almost correspond to planes of indexes (100) and (001), respectively.

The crystal is optically coupled through a 10×20 mm face to a photomultiplier (PMT) ETL mod. 9256B. Its photocathode has an extended green response for a better matching with the light emission spectrum of the CdWO$_4$ crystal. In the measurements with low energy electrons the crystal has been wrapped with Teflon tape, while in measurements under beam an aperture of 10×10 mm has been opened in the tape covering one 20×25 mm face, so that ions can enter directly. It has been verified with γ sources that no measurable difference in light collection is found with or without aperture. The energy scale of the detector was established with ^{22}Na, ^{57}Co, ^{60}Co, ^{137}Cs and ^{241}Am calibration sources.

In all the measurements the anode signals from the PMT are processed by a current-to-voltage converter which acts also as an anti-aliasing filter and analysed by a transient digitiser[2] already described in Ref. [21]. The data, sequentially digitised every 50 ns, are stored in a temporary memory FIFO, which, in the presence of an event trigger, is stopped and read in a time interval starting about 30 μs before the time of the event and extending to 128 μs on the whole. These data are stored on a mass memory for further analysis. In particular, the amplitude spectra are obtained by the following procedure: for each event the mean value of the baseline is evaluated in the first 25 μs and subtracted channel by channel, afterwards the signal amplitude is obtained by summing up the channel contents in a time interval lasting 55 μs from the beginning of the signal. It is also checked whether the analysed waveform is in true or chance coincidence with the event trigger; overlapping waveforms are recognised and discarded.

3. Response to protons, α particles, Li, C, O and Ti ions

3.1. Measurements with pulsed beams

Beams of protons, Li, C, O, and Ti ions, in the energy range 1–10 MeV, were produced by the Tandetron accelerator of LABEC

at the INFN-Florence. A dedicated beam line [22] provides short pulses by means of an electrostatic deflector which displaces the beam spot across a narrow window obtained by an adjustable slits system, housed at the entrance of the vacuum chamber, situated at the end of the beam-line and containing the crystal. The beam intensity and the width of the slits were adjusted to obtain the arrival of a single particle per pulse in a large majority of the cases. As already mentioned in Section 2, in all these measurements the accelerated particles enter the crystal perpendicularly to a 20 mm × 25 mm (001) face. In these measurements the event trigger was derived from the voltage transition of the deflecting plates. Owing to this coincidence constraint on the stored pulse shapes, it is possible to build from them energy spectra almost free from the background. The measured quenching factors for protons (1.0, 2.0, 3.0, 4.0 MeV), Li (3.0, 4.5 MeV), C (3.0, 5.1, 7.5 MeV), O (6.0 MeV) and Ti (10.0 MeV) ions are presented in Fig. 1.

Differences in the pulse shapes, as a consequence of different specific energy losses, have been also investigated.

3.2. Measurements with α particles

In addition to measurements with accelerated ions, the CdWO$_4$ crystal was irradiated with α particles. A collimated ^{241}Am α source was placed, inside the crystal chamber, in front of the crystal (001) face and, at the same time, the crystal was irradiated by ^{137}Cs and ^{60}Co γ sources in order to get a reference γ energy scale. In this case a self-trigger was used and, taking advantage from the different zero-crossing times, α particle and γ ray spectra were easily disentangled. From this measurement the quenching factor for the 5486 keV α particles, entering perpendicularly the (001) face, was found to be 0.127(1) as reported in Fig. 1. In a different series of measurements, the three faces of the bare crystal have been irradiated with α particles. The measured QFs were: 0.197(1) for (010) face, 0.167(1) for (100) face and 0.134(1) for (001) face. These measurements can be helpful for determining the response of the crystal to particles created in its volume and moving in random directions with respect to the principal planes. A comment is required by the small ($\leq 5\%$) but significant difference between the two QF values relative to the (001) face: most probably, the difference could be attributed to the different light losses associated with the different locations of α and γ light emitting sources (a surface point-like light source in the case of α particles and a volume distributed light source in the case of γ rays) with respect to the different reflecting and diffusing properties of the bare and Teflon wrapped crystal.

Difference in QFs for α particles moving in different directions, in addition to CdWO$_4$ detectors (here and e.g. in Ref. [20]) was observed also for ZnWO$_4$ [23] and MgWO$_4$ [24] crystal scintillators. As quenching depends on ionisation density [11], such a behaviour of the QFs has to be related to difference in ionisation density and stopping power for α particles moving in different directions inside an anisotropic crystal. This interpretation is also supported by the behaviour of the shape indicator (Section 3.4), which also depends on the direction of the α particles, being closer to that of γs when the quenching factor is larger. Differences in light collection due to the surface effects could, in fact, change the quenching factor but hardly modify the shape of the light pulse.

3.3. Calculations of quenching factors for ions

Quenching factors Q_i for protons, α particles and Li, C, O, Ti ions in the CdWO$_4$ scintillator were calculated following the work [12], which is based on the classical Birks formula [11], as the ratio of

---
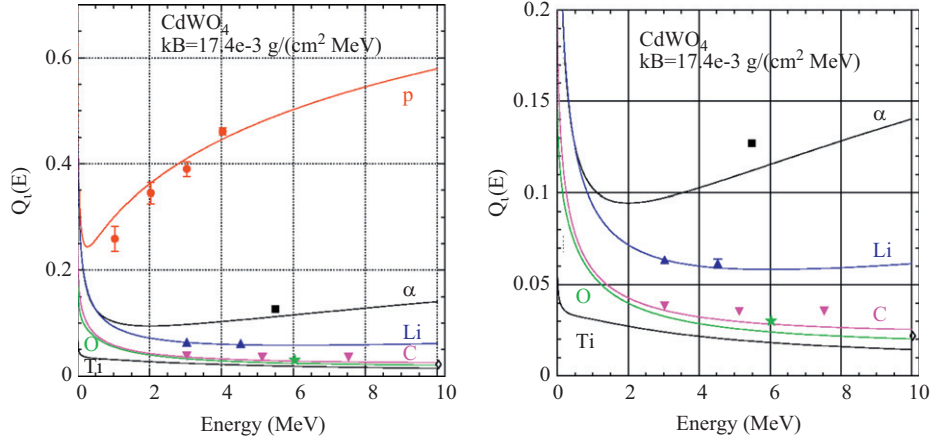
Fig. 1. Quenching factors for protons (•), α particles (■), Li (▲), C (▼), O (⋆) and Ti (◇) ions measured with the CdWO$_4$ crystal scintillator. Solid lines represent calculations in accordance with Ref. [12]. On the right, lower QFs are shown in more detail.

light yield of an ion to that of an electron of the same energy

$$Q_i(E) = L_i(E)/L_e(E) \qquad (1)$$

where

$$L_i(E) = \int_0^E dL_i = \int_0^E \frac{S_i \, dE}{1 + kB\left(\frac{dE}{dr}\right)_i}, \qquad (2)$$

$$L_e(E) = \int_0^E dL_e = \int_0^E \frac{S_e \, dE}{1 + kB\left(\frac{dE}{dr}\right)_e}. \qquad (3)$$

Here $(dE/dr)_i$ and $(dE/dr)_e$ are the total stopping powers for ions calculated with the SRIM code [25] and electrons calculated with the ESTAR code [26], respectively.

Supposing the normalisation factors $S_{i,e}$ equal for electrons and ions and independent on energy, we obtain that $Q_i(E)$ depends only on a single parameter kB (the Birks factor). It is assumed that kB is also independent of energy and has the same value for all ions, if all data are measured under the same experimental conditions and treated in the same way [12].

To determine the kB value for the present CdWO$_4$ measurements, the experimental points for protons were fitted by curve calculated with Eqs. (1)–(3). The result is $kB = 17.4$ mg cm^{-2} MeV^{-1}, and the obtained curve is shown in Fig. 1. Afterwards, QFs for all other ions were calculated with this kB value; all the results are also described in Fig. 1.

As one can see, the calculations do not perfectly reproduce the experimental points, with the biggest deviation ($\simeq 30\%$) for Ti ions. Nevertheless, general agreement could be considered as acceptable, especially for a theory with only one parameter. Sometimes quenching factors in DM experiments are known with much bigger uncertainties, and calculations in accordance with the above-described approach could give valuable information on the expected QF values.

3.4. Pulse-shape discrimination between γ quanta, protons, α particles and light ions

To test the ability of pulse-shape discrimination between γ quanta (β particles), protons, α particles and the light ions, the data were analysed by using the optimal filter method proposed by Gatti and De Martini [27] (see also [28] where the analysis was developed for CdWO$_4$ crystal scintillators). For each experimental signal, its shape indicator was defined as $SI = \sum f(t_k) \times P(t_k)/ \sum f(t_k)$, where the sum is over time channels k, starting from the origin of signal

and up to 60 μs, $f(t_k)$ is the digitised amplitude of a given signal. The weight function $P(t)$ is defined as $P(t) = \bar{f}_\alpha(t) - \bar{f}_\gamma(t)$, where the reference pulse shapes $\bar{f}_\alpha(t)$ and $\bar{f}_\gamma(t)$ are the average of a few thousands shapes for α particles and γ quanta, respectively, collected in the measurements with γ and α sources.

Distributions of the shape indicator versus energy for γ quanta, protons, α particles, Li, C, O and Ti ions measured with CdWO$_4$ crystal scintillator are presented in Fig. 2. There is a clear discrimination between γs, protons, α particles and ions. The shape indicator values for protons and ions lie near the ones of α particles. This fact, however, does not necessarily imply that the pulse shape be equal for heavier ions and protons.

It is worth to note also that the measurements with ^{241}Am α particles entering into different faces of the CdWO$_4$ crystal (Section 3.2) show a clear relation between quenching factor and shape indicator: for bigger QF_α, when α signal is closer to signal caused by γ quanta, SI_α value is lower, i.e. also closer to SI_γ. This effect was already observed in [20,23].

4. Measurements with low energy electrons

It should be noted that the quenching of scintillation signals is observed not only for ions but also for low-energy (less than a few hundred keV) γ quanta and electrons. However, the nature of the electron-induced light-emitting excitation can have a different origin from that induced by heavy ions. Possible relation between QFs for ions and QFs for electrons is interesting and important as giving an additional method to obtain QFs for recoils induced by WIMPs in scintillators.

A lot of work has been dedicated, also recently, to the study of the non-linearity of the response of scintillating crystals, coupled to different types of photo-detectors (photomultipliers in many cases), to low-energy γ quanta and electrons (see e.g. [29–36] and works quoted therein). We have studied the response of a CdWO$_4$ scintillation detector to low energy electrons by using electrons created in the CdWO$_4$ crystal by Compton scattered γ quanta.

4.1. Experimental set-up

To avoid surface effects for low energy electrons, the CdWO$_4$ crystal under study is used as a Compton spectrometer.[3] This technique requires that the γ rays, scattered by the crystal at an

---

[3] This method was first proposed by Valentine and Rooney [37,38].
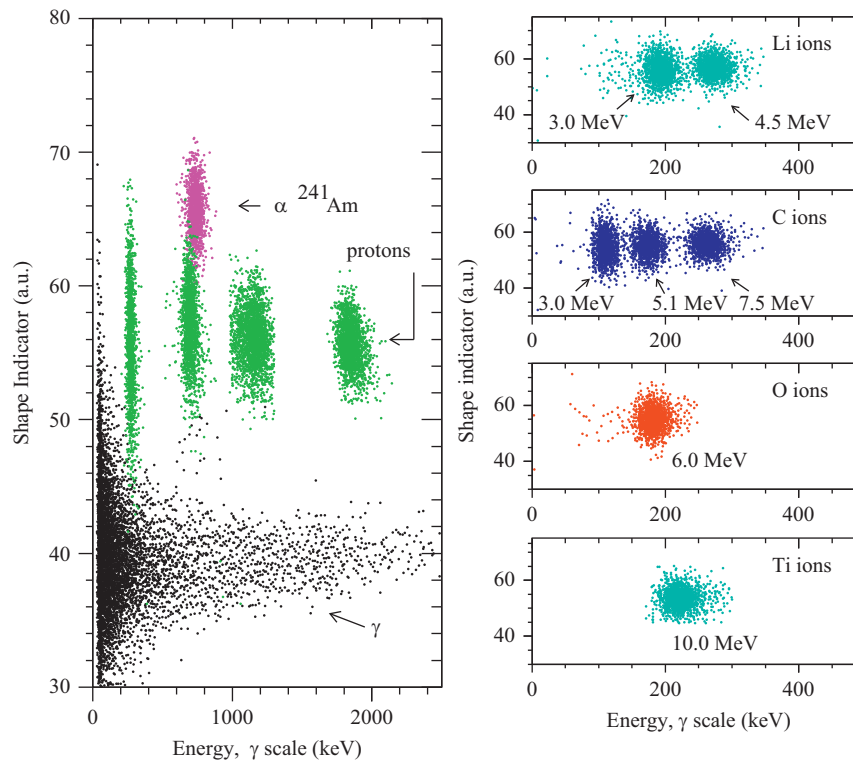
Fig. 2. Distributions of shape indicator (see text) versus energy for protons, Li, C, O and Ti ions measured with the CdWO$_4$ crystal scintillator at the accelerator. Data for γ quanta were obtained from a background run (mainly environmental radioactivity), while α particles were accumulated with the ^{241}Am source installed in the vacuum chamber of the accelerator.

angle θ with respect to the direction of the incoming collimated monochromatic beam, can be detected in coincidence with the signals generated in the crystal by the corresponding scattered electrons. However, when the energy of the scattered electrons is small, typically less than 20 keV, it becomes difficult to achieve reliable information both in energy and in timing, particularly for crystals, such as CdWO$_4$, whose main light emission is characterised by a long decay time (≈ 14 μs) [39]: in that case a small anode signal consists of a sequence of almost randomly spaced single electron responses.

To overcome this problem, we have used the production in opposite directions of the two 511 keV γ rays from the singlet positronium following the β^+ decay of ^{22}Na. This variant of the Compton Coincidence Technique makes it possible to obtain a good timing of the event trigger through the coincidence between one of the γ rays observed by a NaI(Tl) counter and the other one observed in a high purity germanium (HPGe) counter, after been scattered in the crystal under study, and therefore to study the response to electrons down to very low energy also for CdWO$_4$. Moreover the collimation of the γ rays, impinging on the crystal, is performed *via* coincidences with NaI(Tl), so avoiding the border effects of a physical collimator. The front-end electronics for the NaI(Tl) detector consists of a passive integrator of the anode current signals followed by a JFET input linear buffer feeding a semi-gaussian shaping amplifier (Ortec, mod. 572: time constant 0.5 μs) whose bipolar output is sent to a Timing Single-Channel Analyzer (Ortec, mod. 551). HPGe signals, from one of the twin outputs of the charge preamplifier, are processed in the same way as those of the NaI(Tl) detector and provide timing information, while the other preamplifier output is connected to a Gated Integrator Amplifier (Ortec, mod. 973) with integration time 5 μs, and used for energy measurement.

The geometry of the experimental set-up is shown in Fig. 3. The ^{22}Na source has nominal activity 400 kBq. ^{22}Na decays to the
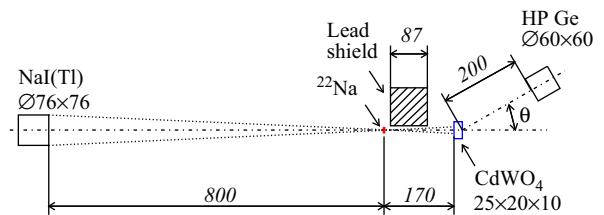
Fig. 3. Set-up for measurements of CdWO$_4$ crystal scintillator response to low energy electrons. All sizes are in mm. The angle θ has been set to 12.5°, 20° and 35°. The Al cap surrounding the CdWO$_4$ crystal is not shown.

1274.5 keV, first excited level of ^{22}Ne, through a β^+ ($E_{max}=546$ keV) annihilating in a 2 mm diameter zone.

As shown in Fig. 3, the source is on the axis of a system of two detectors: a $3'' \times 3''$ NaI(Tl) (manufactured by Scionix) and the CdWO$_4$ crystal described in Section 2. The 10 mm thickness of this crystal causes an attenuation of the 511 keV γ rays of $\approx 60\%$. Special care has been devoted to minimise the material surrounding the CdWO$_4$ crystal and thus the probability of absorption and scattering along the path of the 511 keV γ rays: to this purpose the cap surrounding the CdWO$_4$ is a cylinder of aluminium of only 0.4 mm thickness. The 800 mm distance between source and front face of the NaI(Tl) detector defines a solid angle of maximum angular aperture of 5.4°, so that a 511 keV γ ray impinging on this detector has a companion 511 keV γ ray hitting the CdWO$_4$ crystal inside a circle of 16 mm diameter.

The 511 keV γ rays scattered at angle θ from the crystal are detected by an HPGe detector (Ortec: mod. GMX 30 P: diameter 60 mm, height 60 mm, relative efficiency 30% and resolution (FWHM) 1.9 keV at 1.33 MeV). The HPGe detector is placed at ≈ 200 mm from the centre of the crystal and, in successive measurements, at angles θ of (12.5, 20.0, 35.0)° with respect to the axis defined by the NaI(Tl) detector and the CdWO$_4$ crystal. In

this way, the overall angular range covered by the HPGe extends, with variable efficiency, from 0.5° to 44°, corresponding to energies of the scattered γ rays from 510 keV to 395 keV and a complementary energy range of Compton electrons inside the $CdWO_4$ from 1 keV to 116 keV.

It is worth to stress that with this set-up the problem of the time mark associated to even very low energy events in the crystal is overcome, because the event trigger is obtained from the coincidence of 511 keV full-energy signals detected by the NaI(Tl) and signals detected by the HPGe in the energy range (390–511) keV. A drawback of this method concerns the intrinsic energy spread of the 511 keV γ rays, which brings the FWHM of the 511 keV line to ≈ 3.0 keV (the intrinsic HPGe resolution at this energy is ≈ 1.7 keV).

For monitoring gain and baseline of the HPGe, a ^{133}Ba source is placed near the HPGe detector and shielded by a 25 mm lead shield from the $CdWO_4$ crystal. For the same purpose, a source of ^{241}Am (emitting 60 keV photons) is placed near the $CdWO_4$. Lead shields have been also introduced which, to some extent, prevent 511 keV (and to a lesser extent 1274.5 keV) γ rays from the ^{22}Na source, from directly reaching the HPGe detector.

At the arrival of an event trigger, the linear signal from HPGe is peak analysed (by a 100 MHz, 8k ADC) and recorded, together with the information on $CdWO_4$ "signal shape", on a dedicated PC. As an example, the relevant part (470 keV–520 keV) of the HPGe spectrum corresponding to γ rays scattered from the $CdWO_4$ crystal in a 4-days run (corresponding to about one tenth of the total statistics) at a mean angle $\theta = 12.5°$, is shown in Fig. 4a. The broad structure ("bump") in the γ spectrum is due to 511 keV γs Compton scattered in the crystal, which are in prompt coincidence with the event trigger. The out-of-coincidence spectrum (Fig. 4a) clearly shows a 511 keV full energy peak, which is

followed (because of multiple scattering) by a small tail extending from the full-energy peak down to the Compton edge. Obviously, a distribution of the same relative size is present at the low energy side of each channel of the bump and the combined effect of all channels produces the low-energy tail extending well below the minimum energy of the scattered γs. This effect certainly contributes, with increasing importance, to the lower-energy part of the bump. Owing to this reason, only the upper part of the bump has been considered in the analysis.

In Fig. 4b, the corresponding digitiser pulse amplitude spectrum of electrons in prompt coincidence is reported. The nominal energy scale ("apparent electron energy" $\tilde{E}_e$) is normalised to the full-energy peak of 511 keV, corresponding to a full absorption of the γ inside the crystal. Due to the non-linear response, the energy scale does not reproduce the true energy of low-energy electrons.

The small rise in the electron spectrum at the lowest energies is completely accounted for by the background distribution (see the out-of-coincidence spectrum in Fig. 4b).

Within the statistical uncertainties, the energy of electrons associated with a γ ray of energy E_γ is $E_e = 511$ keV$-E_\gamma$. The bump in the distribution of E_γ, shown in Fig. 4a, as well as those at $\theta = 20°$ and $35°$, have been divided into bins 2 or 4 keV wide, and for each bin the distribution of electron signal amplitudes from $CdWO_4$ has been obtained. Examples of the amplitude spectra of electrons are presented in Fig. 5 for mean energies 5.1 keV and 19.1 keV (from 2-keV bins), and 92 keV (4-keV bin). Also in this figure, the electron pulse amplitude has been converted in keV to give the "apparent electron energy" $\tilde{E}_e$. For each amplitude distribution, two values of the mean energy are given in the figure: the true mean energy of the scattered electrons $\langle E_e \rangle = 511$ keV$-\langle E_\gamma \rangle$, coming from the mean value $\langle E_\gamma \rangle$ of the γ energy of the selected bin on the γ bump, and the mean of the apparent electron energy $\langle \tilde{E}_e \rangle$.

Distributions, as those shown in Fig. 5, have been used for two purposes:

(1) from each electron distribution the value of FWHM has been extracted and compared with those obtained by irradiating the $CdWO_4$ crystal with γ rays of similar energies from radioactive sources and
(2) for each bin of the selected regions of the three γ bumps (at $\theta = 12.5°$, $20°$, $35°$) the relative light yield $\langle \tilde{E}_e/E_e \rangle$ of the corresponding electron energy distribution has been evaluated.
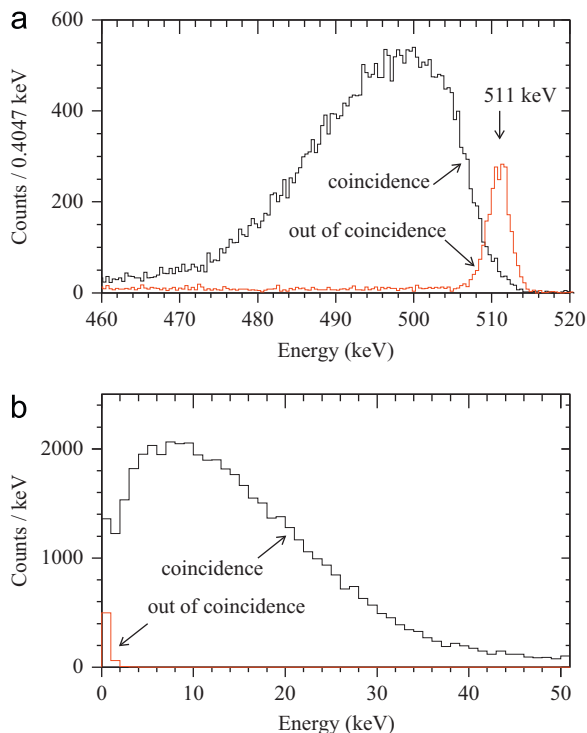
Fig. 4. (a) Spectrum of the 511 keV γ rays scattered by the $CdWO_4$ crystal, acquired by HPGe in prompt coincidence with the corresponding 511 keV γ rays, detected by the NaI(Tl) crystal. The two spectra are normalised to equal time intervals; the latter is then multiplied by 20. (b) Distribution of pulse amplitudes from $CdWO_4$ converted to "apparent electron energy" in keV triggered by the prompt coincidence between HPGe and NaI(Tl); and out of coincidence normalised to equal time intervals. All the spectra refer to mean angle $\theta = 12.5°$ (see Fig. 3).
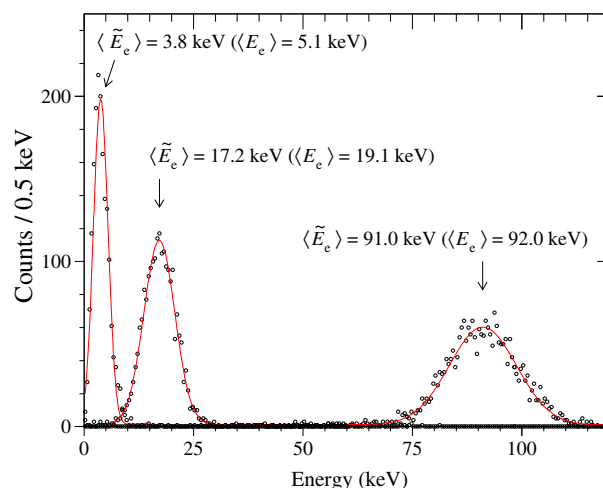
Fig. 5. Energy spectra of electrons with energies 5.1, 19.1 and 92.0 keV measured by $CdWO_4$ crystal scintillator. The solid lines represent the fit to the distributions by a Gaussian function.

4.2. Response of CdWO$_4$ crystal scintillator to low energy electrons

The dependence of the energy resolution on energy of electrons and γs from radioactive sources in CdWO$_4$ is reported as a function of energy in Fig. 6. The main findings are that no appreciable differences between electrons and γ rays are apparent in the overlapping energy region. The continuous line shows a minimum-χ^2 fit of the data with the function FWHM(%) $= \sqrt{a/E}$; ($a = 38\,200 \pm 400$ keV, $\chi^2/$n.d.f. $= 0.45$, where n.d.f. is the number of degrees of freedom).

Concerning the relative light yield, examples of distributions of the ratios $\tilde{E}_e/E_e$, for the same energy bins of Fig. 5, are given in Fig. 7. From this type of distributions, and for each 4-keV bin in the HPGe bumps at angles θ of (12.5, 20.0, 35.0)$^\circ$, the relative light yield is derived as $R = \langle \tilde{E}_e/E_e \rangle$. They are presented as a function of the true electron energy in Fig. 8. Error bars include the statistical uncertainties as well as estimated systematic errors related to the measurement itself and to the procedure of data analysis. The relative light yield remains substantially stable at the 100% value above 80 keV, decreases slowly at lower energies down to 95% at 20 keV and more deeply below this energy.

In CdWO$_4$, no indication is found with an increase in the luminescence efficiency with decreasing electron energy, as reported for NaI(Tl). To our knowledge, no previous measurements
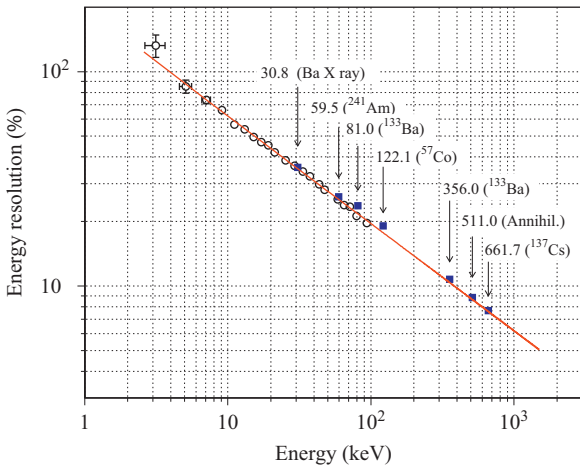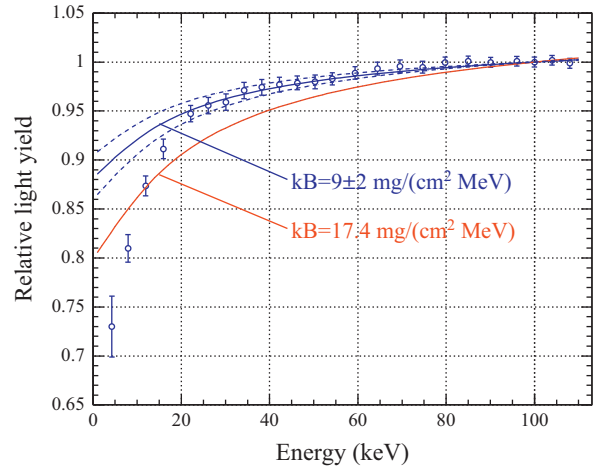

Fig. 8. Relative light yield (normalised to 1 at 100 keV) as a function of the electron energy. Lines show calculations with Eq. (4) with different kB values.

with internal electrons have been reported for CdWO$_4$. Compared with Fig. 10 of Ref. [30], our Fig. 8 shows a slower decrease in the R for energies below 80 keV. We must remark, however, that the data of [30] are obtained by excitation with γ rays, and show in fact the well-known anomalies at the K edge.

We also calculate here the relative light yield as

$$R = L_e(E)/E \qquad (4)$$

with L_e obtained with Eq. (3) and the Birks factor $kB = 17.4$ mg cm^{-2} MeV^{-1}, the same as was used to describe the experimental data for ions (Fig. 1); R is normalised to 1 at 100 keV. However, as one can see from Fig. 8, the experimental data for electrons are better described with the value $kB = 9.0$ mg cm^{-2} MeV^{-1}, when the points at $E > 20$ keV are perfectly described, while disagreement still is present at lower energies. One could expect that introduction of kB dependent on energy (see [40–42]) or introduction of additional terms in the Birks equation (see e.g. [43]) would allow us to improve the description of the data.

5. Discussion and conclusions

(1) It should be stressed that the non-proportionality in the scintillation response is an important characteristic to estimate the energy resolution achievable with scintillation crystals [30]. In accordance with the current understanding (see recent reviews [33–35]), non-proportionality of the relative light yield for electrons and γ quanta at low energies is one of the main reasons of poor energy resolution of a scintillator for γs even at higher energies because of a high probability for a γ quantum to interact with a detector more than once and to lose the total energy through creation of few lower energy electrons. Many scintillating materials were studied till now (see [33–36,44–46] and references therein), and the best energy resolution (better that 3%) was reached with scintillators that show good proportionality of the light yield down to $\simeq 10$ keV (e.g. LaCl$_3$(Ce), LaBr$_3$(Ce), SrI$_2$(Eu) [35]). While response of CdWO$_4$ to low energy γ quanta was already studied [30,45], results for low energy electrons (down to 5 keV) are presented here for the first time.

(2) Measurements with the accelerator for protons, Li, C, O and Ti ions with energies in 1–10 MeV interval, together with the 5.5 MeV α particles from ^{241}Am, allow us to obtain data on quenching factors interesting for the dark matter studies. Description of these data with Eqs. (1)–(3) with the same value of the Birks factor $kB = 17.4$ mg cm^{-2} MeV^{-1} (obtained by fitting the data for protons), while being not perfect, nevertheless shows relevant agreement, with the

Fig. 6. FWHM of the distributions of pulse amplitudes from the CdWO$_4$ counter for Compton electrons and γs from various radioactive sources.
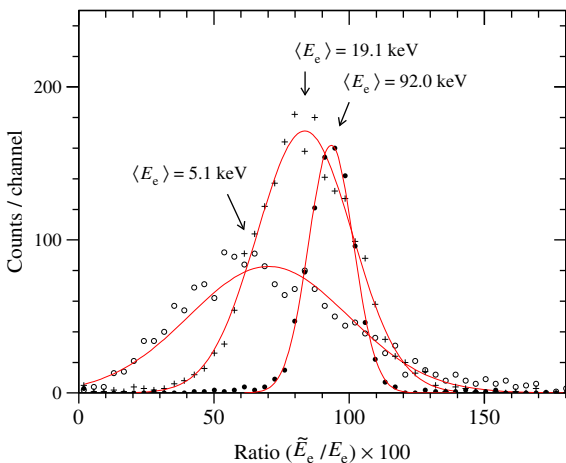

Fig. 7. Examples of distributions of ratio $\tilde{E}_e/E_e$ of the CdWO$_4$ scintillation response together with their fits by a Gaussian function.

biggest deviation of $\simeq 30\%$ for Ti ions. This further supports the hypothesis [12] that quenching factors for all ions are not independent and could be described with the same kB value, if the data are collected in the same experimental conditions and are treated in the same way. This approach allows us to obtain QFs for low energy nuclear recoils on the basis f.e. of QFs values for a few MeV α particles from internal contamination of a detector. Sometimes the QFs for low energy nuclear recoils are known with uncertainties much higher than 30%, and the description with Eqs. (1)–(3) could provide an important estimation of the needed QFs.

(3) It is possible to describe the obtained data on the relative light yield for low energy electrons in CdWO$_4$ by Eq. (4) in a perfect way for $E > 20$ keV, however still with disagreement at lower energies. Similar description on the basis of the Birks equation was obtained previously for CaWO$_4$ in Ref. [47] and for liquid scintillators in the Double Chooz experiment in Ref. [48]. However, for CdWO$_4$ the value $kB = 9.0$ mg cm^{-2} MeV^{-1} determined for such a description is different from that obtained from fit of the data for the ions: $kB = 17.4$ mg cm^{-2} MeV^{-1}. This unfortunately closes the additional way to obtain QFs for low energy nuclear recoils relevant for the DM searches from the light yield non-proportionality for the electrons measured with the same scintillator. This conclusion is not unexpected; it is supported also by the following considerations. As it is known (see f.e. [35]), for some scintillating materials (NaI(Tl), CsI(Tl)) the relative light yield for γ quanta and electrons is $R > 1$ at low energies. At the same time, Eq. (4) can describe only quenched values $R < 1$ (as those in Fig. 8 or in Refs. [47,48]) but not the enhanced $R > 1$ (giving at most only $R = 1$ with $kB = 0$), thus it is not suitable for NaI(Tl). One could assume that the mechanisms of quenching for ions and non-linear response to low energy electrons (γs) are different. Nevertheless, description for ions by Eqs. (1)–(3) is valid also for NaI(Tl); see f.e. Fig. 13a in Ref. [12] where the kB value obtained by fitting data for Na recoils allowed us to perfectly describe QFs for I recoils.

Acknowledgements

References

[1] J.L. Feng, Annual Review of Astronomy and Astrophysics 48 (2010) 495.
[2] G. Bertone (Ed.), Particle Dark Matter. Observations, Models and Searches, Cambridge University Press, 2010.
[3] R. Bernabei, et al., European Physical Journal C 56 (2008) 333;
R. Bernabei, et al., European Physical Journal C 67 (2010) 39.
[4] C. Aalseth, et al., Physical Review Letters 107 (2011) 141301.
[5] G. Angloher, et al., European Physical Journal C 72 (2012) 1971.
[6] N.J.C. Spooner, Journal of the Physical Society of Japan 76 (2007) 111016.
[7] W. Rau, Physics of Particles and Nuclei 42 (2011) 650.
[8] H. Kraus, et al., Nuclear Physics B (Proceedings Supplements) 173 (2007) 168.
[9] L. Baudis, et al., arXiv:1201.2402 [astro-ph.IM].
[10] F. Cappella, et al., Nuovo Cimento B 122 (2007) 707.
[11] J.B. Birks, The Theory and Practice of Scintillation Counting, Pergamon Press, Oxford, 1964.
[12] V.I. Tretyak, Astroparticle Physics 33 (2010) 40.
[13] F.A. Danevich, et al., Zeitschrift für Physik A 355 (1996) 433.
[14] F.A. Danevich, et al., Physical Review C 68 (2003) 035501.
[15] P. Belli, et al., European Physical Journal A 36 (2008) 167.
[16] A.S. Barabash, et al., Journal of Instrumentation 06 (2011) P08011.
[17] P. Belli, et al., Physical Review C 85 (2012) 044610.
[18] F.A. Danevich, et al., Physics of Atomic Nuclei 59 (1996) 1.
[19] P. Belli, et al., Physical Review C 76 (2007) 064603.
[20] F.A. Danevich, et al., Physical Review C 67 (2003) 014310.
[21] L. Bardelli, et al., Nuclear Instruments and Methods in Physics Research Section A 569 (2006) 743.
[22] N. Taccetti, et al., Nuclear Instruments and Methods in Physics Research Section B 188 (2002) 255.
[23] F.A. Danevich, et al., Nuclear Instruments and Methods in Physics Research Section A 544 (2005) 553.
[24] F.A. Danevich, et al., Nuclear Instruments and Methods in Physics Research Section A 608 (2009) 107.
[25] J.F. Ziegler, J.P. Biersack, M.D. Ziegler, SRIM. The Stopping and Range of Ions in Matter, SRIM Co., 2008;
SRIM Version 2008.04, ⟨http://www.srim.org⟩.
[26] M.J. Berger, J.S. Coursey, M.A. Zucker, J. Chang, Stopping-Power and Range Tables for Electrons, Protons, and Helium Ions, Version 1.2, ⟨http://physics.nist.gov/PhysRefData/Star/Text/contents.html⟩.
[27] E. Gatti, F. De Martini, Nuclear Electronics 2, IAEA, Vienna, 1962, p. 265.
[28] T. Fazzini, et al., Nuclear Instruments and Methods in Physics Research Section A 410 (1998) 213.
[29] E. Sakai, IEEE Transactions on Nuclear Science NS-34 (1987) 418.
[30] P. Dorenbos, J.T.M. de Haas, C.W.E. van Eijk, IEEE Transactions on Nuclear Science NS-42 (1995) 2190.
[31] J.E. Jaffe, D.V. Jordan, A.J. Peurrung, Nuclear Instruments and Methods in Physics Research Section A 570 (2007) 72.
[32] W.S. Choong, et al., IEEE Transactions on Nuclear Science NS-55 (2008) 1073.
[33] S.A. Payne, et al., IEEE Transactions on Nuclear Science NS-56 (2009) 2506.
[34] M. Moszyński, Radiation Measurements 45 (2010) 372.
[35] S.A. Payne, et al., IEEE Transactions on Nuclear Science NS-58 (2011) 3392.
[36] I.V. Khodyuk, P. Dorenbos, arXiv:1204.4350 [cond-mat.mtrl-sci].
[37] J.D. Valentine, B.D. Rooney, Nuclear Instruments and Methods in Physics Research Section A 353 (1994) 37.
[38] B.D. Rooney, J.D. Valentine, IEEE Transactions on Nuclear Science NS-43 (1996) 1271.
[39] L. Bardelli, et al., Nuclear Instruments and Methods in Physics Research Section A 584 (2008) 129.
[40] G. Bizarri, et al., Journal of Applied Physics 105 (2009) 044507.
[41] Q. Li, et al., Journal of Applied Physics 109 (2011) 123716.
[42] R.T. Williams, et al., Physica Status Solidi B 248 (2011) 426.
[43] C.N. Chou, Physical Review 87 (1952) 904.
[44] M. Moszyński, Nuclear Instruments and Methods in Physics Research Section A 505 (2003) 101.
[45] M. Moszyński, IEEE Transactions on Nuclear Science NS-52 (2005) 3124.
[46] G. Bizarri, et al., Journal of Luminescence 129 (2009) 1790.
[47] R.F. Lang, et al., arxiv:0910.4414 [nucl-ex].
[48] C. Aberle, et al., Journal of Instrumentation 6 (2011) P11006.